

Bose-Hubbard phase diagram with arbitrary integer filling

Niklas Teichmann,^{*} Dennis Hinrichs, and Martin Holthaus
Institut für Physik, Carl von Ossietzky Universität, D-26111 Oldenburg, Germany

André Eckardt
Institut de Ciències Fotòniques (ICFO), E-08860 Castelldefels (Barcelona), Spain

(Received 16 January 2009; published 6 March 2009)

We study the transition from a Mott insulator to a superfluid in both the two- and the three-dimensional Bose-Hubbard model at zero temperature, employing the method of the effective potential. Converting Kato's perturbation series into an algorithm capable of reaching high orders, we obtain accurate critical parameters for any integer filling factor. Our technique allows us to monitor both the approach to the mean-field limit by considering spatial dimensionalities $d > 3$ and to the quantum rotor limit of high filling, which refers to an array of Josephson junctions.

DOI: [10.1103/PhysRevB.79.100503](https://doi.org/10.1103/PhysRevB.79.100503)

PACS number(s): 67.85.Hj, 03.75.Hh, 03.75.Lm, 64.70.Tg

The Bose-Hubbard model, describing interacting Bose particles moving on a tight-binding lattice, has drawn much attention, especially after its experimental realization with ultracold bosonic atoms in optical potentials (see Ref. 1 and references therein). This clean defectless setup, which allows for precise control of its parameters, has opened up testing ground for quantum many-body physics. The pure Bose-Hubbard system reflects the competition between the potential energy due to the repulsive on-site interaction among the Bosons, which tends to suppress density fluctuations and to localize the particles, and the kinetic energy associated with tunneling processes between neighboring lattice sites, which try to delocalize the particles and to reduce phase fluctuations. Denoting the on-site interaction energy of a pair of particles sitting at the same site by U , and the hopping matrix element by J , the model's grand-canonical Hamiltonian is written in dimensionless form as²

$$H_{\text{BH}} = \underbrace{\frac{1}{2} \sum_j \hat{n}_j (\hat{n}_j - 1)}_{H_0} - \mu/U \sum_j \hat{n}_j - \underbrace{J/U \sum_{\langle j,k \rangle} \hat{a}_j^\dagger \hat{a}_k}_{H_{\text{tun}}}, \quad (1)$$

where indices label the sites of a d -dimensional lattice, which we take as hypercubic, and the sum over $\langle j, k \rangle$ extends over nearest neighbors. As usual, \hat{a}_j^\dagger and \hat{a}_j are the creation and annihilation operators for a Boson at site j , and $\hat{n}_j = \hat{a}_j^\dagger \hat{a}_j$ is the number operator at that site. The chemical potential μ here is site independent. At zero temperature one finds a series of Mott phases at sufficiently small values of J/U , characterized by a fixed filling of an integer number of particles per site, depending on the value of μ/U . A Mott state has zero compressibility, due to an energy gap separating the ground state from the particle and hole excitations, so that it costs energy to move a particle through the system. Upon increasing the ratio J/U , the competition between potential and kinetic energies leads to a quantum phase transition: at the phase boundary $(J/U)_{\text{pb}}$ the gap closes so that particle delocalization becomes favorable and the system

Bose condenses into a superfluid state for $d \geq 2$.² In optical lattice experiments performed so far, this transition has been induced by varying the lattice depth,³ as in the pioneering work by Greiner *et al.*,⁴ and by shaking the lattice periodically in time with slowly varying amplitude,⁵ as done recently by Zenesini *et al.*⁶

Despite the apparent simplicity of Hamiltonian (1), a precise calculation of its critical parameters for different dimensionalities d and filling factors g poses severe challenges so that the determination of the phase diagram in the $J/U - \mu/U$ plane has become a major benchmark problem for computational many-body physics. Recent quantum Monte Carlo (QMC) simulations have yielded critical parameters with record accuracy for $g=1$.^{7,8} A previous strong-coupling expansion had led to reliable analytical results to third order in J/U (Ref. 9) and later was extended to higher orders in one and two dimensions (2D) for $g=1$ and $g=2$.¹⁰ Techniques using the density-matrix renormalization group (DMRG) allow one to treat fairly large systems in one dimension¹¹⁻¹³ but up to now have remained restricted to low filling. So far, accurate critical data for the three-dimensional (3D) system with experimentally relevant higher filling factors $g > 1$ have remained particularly hard to obtain.

In this contribution we show that a specific adaption of high-order many-body perturbation theory, based on Kato's formulation of the perturbation series^{14,15} and using the concept of the order parameter, enables one to investigate Bose-Hubbard systems with arbitrary integer filling factor. In principle, the technique is applicable to any type of lattice in any dimension. We first briefly sketch the method and present our results for both 2D and 3D lattices. We then numerically monitor the approach to the mean-field limit of high lattice dimension and to the quantum rotor limit of high filling,^{16,17} which describes a Josephson junction array.¹⁸

Our starting point is the method of the effective potential,¹⁹ as considered recently by dos Santos and Pelster.²⁰ Adding source terms to the Bose-Hubbard Hamiltonian (1), which attempt to add particles with uniform strength χ to each site or to remove them with strength χ^* according to

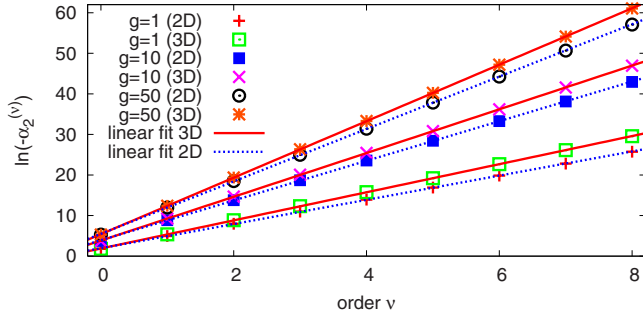


FIG. 1. (Color online) Logarithm of the coefficients $-\alpha_2^{(\nu)}$ for filling factors $g=1, 10$, and 50 in two and three dimensions, with linear fits. The chemical potential is chosen as $\mu/U=g-0.5$.

$$\tilde{H}_{\text{BH}}(\chi, \chi^*) = H_0 + H_{\text{tun}} + \sum_j (\chi^* \hat{a}_j + \chi \hat{a}_j^\dagger), \quad (2)$$

then expanding the grand-canonical free energy $F = \langle \tilde{H}_{\text{BH}} \rangle$ at zero temperature into a power series in the hopping parameter J/U and the sources χ and χ^* , one has

$$F(J/U, \chi, \chi^*) = M \left(F_0(J/U) + \sum_n c_{2n}(J/U) |\chi|^{2n} \right) \quad (3)$$

for a lattice of M sites, with coefficients

$$c_{2n}(J/U) = \sum_\nu \alpha_{2n}^{(\nu)}(J/U)^\nu. \quad (4)$$

The order parameter ψ now specifies the change in F in response to a variation in the sources,

$$\psi = \langle \hat{a}_j \rangle = \frac{1}{M} \frac{\partial F}{\partial \chi^*} \quad \text{and} \quad \psi^* = \langle \hat{a}_j^\dagger \rangle = \frac{1}{M} \frac{\partial F}{\partial \chi}, \quad (5)$$

while the effective potential $\Gamma = F/M - \psi^* \chi - \psi \chi^*$ is the Legendre transform of F , with ψ and ψ^* as independent variables. With the help of Eqs. (5) and (3) one gets the familiar Landau form

$$\Gamma(J/U, \psi, \psi^*) = F_0 - \frac{1}{c_2} |\psi|^2 + \frac{c_4}{c_2} |\psi|^4 + \dots \quad (6)$$

Since $\partial \Gamma / \partial \psi = -\chi^*$ and $\partial \Gamma / \partial \psi^* = -\chi$, and since the original Bose-Hubbard system is recovered by setting $\chi = \chi^* = 0$, the system adopts that order parameter which minimizes Γ . Unless μ/U is an integer, one has $c_2 < 0$ for sufficiently small J/U whereas $c_4 > 0$ so that one finds a Mott regime with $\psi = 0$. Upon increasing J/U , the system enters the superfluid phase when ψ acquires a nonzero value, indicating long-range phase coherence. Hence, the phase boundary is determined by that J/U for which the minimum of expression (6) starts to deviate from $|\psi|^2 = 0$, which occurs when the coefficient $-1/c_2$ of $|\psi|^2$ vanishes. In effect, one has to identify that scaled hopping strength J/U for which the susceptibility c_2 diverges; this divergence marks the quantum phase transition.²⁰

For computing c_2 we resort to Kato's formulation of the perturbation series,^{14,15} starting from the site-diagonal Hamiltonian H_0 . For integer filling factor g , its ground state $|\mathbf{m}\rangle$ is a product of local Fock states with g particles sitting at

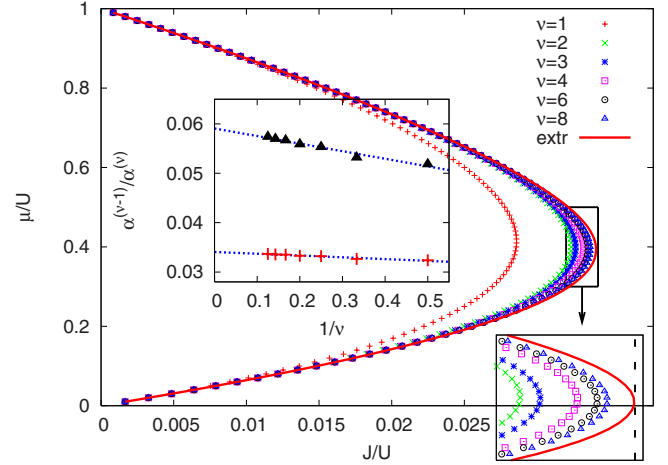


FIG. 2. (Color online) Phase boundary for the 3D model with unit filling, as determined from the ratios $\alpha^{(\nu-1)}/\alpha^{(\nu)}$ for finite orders ν , together with the extrapolation to $\nu = \infty$ (extr). The inset at the right bottom magnifies the tip of the lobe, and demonstrates the convergence to the QMC result (Ref. 7) (dashed vertical line). The central inset illustrates the extrapolation of $\alpha^{(\nu-1)}/\alpha^{(\nu)}$ to $(J/U)_c$ for $d=2$ (upper data) and $d=3$ (lower data). Observe that the data for $d=3$ fluctuate less.

each site. In general, when the system is subjected to some perturbation V , the n th order correction to its energy is given by the trace¹⁴

$$E_{|\mathbf{m}\rangle}^{(n)} = \text{tr} \left[\sum_{\{\alpha_\ell\}} S^{\alpha_1} V S^{\alpha_2} V S^{\alpha_3} \dots S^{\alpha_n} V S^{\alpha_{n+1}} \right], \quad (7)$$

where the sum runs over all possible sets of non-negative integers α_ℓ which obey $\sum_\ell \alpha_\ell = n-1$. The operators S^α are defined by

$$S^\alpha = \begin{cases} -|\mathbf{m}\rangle \langle \mathbf{m}| & \text{for } \alpha = 0 \\ \sum_{i \neq \mathbf{m}} \frac{|i\rangle \langle i|}{(E_{\mathbf{m}} - E_i)^\alpha} & \text{for } \alpha > 0 \end{cases}, \quad (8)$$

with $E_{\mathbf{m}}$ and E_i denoting the unperturbed energies of the H_0 eigenstates $|\mathbf{m}\rangle$ and $|i\rangle$, respectively. Expression (7) can be understood as a sum over chains of processes mediated by the operators V . Each process chain leads from the Mott-insulator state $|\mathbf{m}\rangle$ over different intermediate states $|i\rangle$ back to $|\mathbf{m}\rangle$. Such chains can be represented by abstract diagrams, with only connected diagrams contributing to the sum, as stated by the linked-cluster theorem.²¹ Each diagram has a certain weight depending on the lattice's type and dimensionality. For example, diagrams for the energy correction due to tunneling consist merely of closed loops of individual tunneling processes. In contrast, for calculating c_2 the augmented Hamiltonian (2) prompts us to set

$$V = -J/U \sum_{\langle j,k \rangle} \hat{a}_j^\dagger \hat{a}_k + \sum_j (\chi^* \hat{a}_j + \chi \hat{a}_j^\dagger). \quad (9)$$

Because we are aiming at the coefficient of $|\chi|^2$ in Eq. (3), we only need to take into account terms containing exactly one creation and one annihilation process. This selection yields $c_2(J/U) = \sum_\nu \alpha_2^{(\nu)}(J/U)^\nu$ as a series in the tunneling pa-

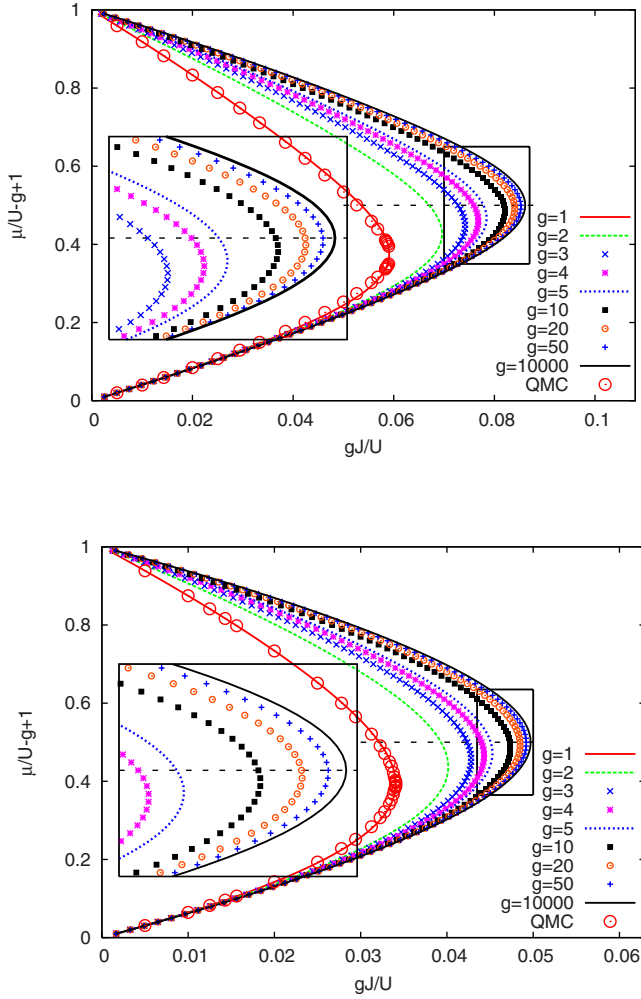


FIG. 3. (Color online) Mott lobes for $d=2$ (upper panel) and $d=3$ (below) with various g . Dashed lines mark the quantum rotor limit $(\mu/U)_c = g - 0.5$ of the critical chemical potential. The lobes' tips are magnified in the inset, illustrating the convergence of $g(J/U)_c$. For unit filling, QMC data (Refs. 7 and 8) are included.

parameter J/U . The only relevant third-order diagram thus consists of one creation of a Boson (\bullet), one tunneling process (\rightarrow), and one annihilation (\times). The fourth-order diagrams then read as

$$\bullet \rightarrow \rightarrow \times, \quad \bullet \times \rightleftharpoons, \quad (10)$$

with the second diagram indicating chains for which creation and annihilation take place at the same site. The computational effort increases quickly with the order: for $\nu=8$, say, all permutations of up to ten different processes ($8 \rightarrow, 1 \bullet, 1 \times$) encoded in the diagrams have to be evaluated.

An instructive example for illustrating this scheme occurs in the limit of infinite lattice dimensionality d . Here the diagrams containing “back and forth” tunneling processes [analogous to second diagram (10)] do not contribute to the sum because they acquire vanishing weight for $d \rightarrow \infty$. The remaining diagrams simply are

$$\bullet \times, \bullet \rightarrow \times, \bullet \rightarrow \rightarrow \times, \dots, \bullet \rightarrow \rightarrow \dots \rightarrow \times. \quad (11)$$

Being one-particle reducible, they factorize into their one-particle irreducible contributions^{20,22}

$$\begin{aligned} \bullet \rightarrow \times &= (-1)(\bullet \times)^2 \\ \bullet \rightarrow \rightarrow \times &= (-1)^2(\bullet \times)^3 \\ &\vdots \\ \bullet (\rightarrow)^\nu \times &= (-1)^\nu (\bullet \times)^{\nu+1}. \end{aligned} \quad (12)$$

For each tunneling process one has an additional factor $2d$ since there exist $2d$ directions on a d -dimensional rectangular lattice. The resulting series for $c_2(J/U)$ is geometric because $\alpha_2^{(\nu-1)}/\alpha_2^{(\nu)} = -1/(2d\alpha_2^{(0)})$ is constant; this ratio determines its radius of convergence and hence directly gives the phase boundary as follows:

$$2d(J/U)_{\text{pb}} = \frac{(g - \mu/U)(\mu/U - g + 1)}{\mu/U + 1}, \quad (13)$$

which is precisely the mean-field result.^{2,16}

We have devised an algorithm for efficiently generating and evaluating all diagrams up to some order for any lattice dimension d . In two and three dimensions we obtain (negative) coefficients $\alpha_2^{(\nu)}$ which form almost perfect geometric series, as depicted in Fig. 1 for $g=1, 10$, and 50 . If the ratio $\alpha_2^{(\nu-1)}/\alpha_2^{(\nu)}$ was constant, it would equal the phase boundary as in the example above. But since now this ratio changes slightly with the number ν of tunneling processes taken into account, we carry out an extrapolation over $1/\nu$ by making a linear fit based on the orders 1–8 in J/U (3–10 in V), as illustrated by the central inset in Fig. 2. Different selections of the orders employed (e.g., 2–8 in J/U) lead to very similar results, with an uncertainty of about 1% in 3D and 2% in 2D. The main part of Fig. 2 shows the phase boundary thus obtained for the 3D case at unit filling, together with some approximants for finite orders. The tip of the lobe corresponds to the critical parameter $(J/U)_c$ for which QMC calculations have provided a highly accurate reference value: $(J/U)_c = 0.034\,08(2)$ for $g=1$.⁷ Our data match this value fairly well, as emphasized by the lower right inset.

Critical parameters obtained for higher filling g in two and three dimensions are collected in Table I. With increasing g , the critical chemical potential $(\mu/U)_c$ approaches $g - 0.5$ due to the fact that there is exact particle-hole symmetry for $g \rightarrow \infty$. Some corresponding Mott lobes are depicted in Fig. 3; for $g=1$, QMC data^{7,8} are included for comparison.

Our technique permits us to reach higher dimensionalities $d > 3$, thus uncovering how the mean-field limit is approached, and high filling factors $g \gg 1$. In the latter regime, the phases at the individual sites become well defined so that the Bose-Hubbard model reduces to a quantum rotor model containing a single parameter gJ/U and describing a Josephson junction array.^{16,18} Figure 4 indeed reveals that the products $2dg(J/U)_c$ remain almost constant when g exceeds 100,

TABLE I. Critical values $(\mu/U)_c$ and $(J/U)_c$ for various filling factors g . For locating the tip of the respective Mott lobe, μ/U has been varied in steps of 0.001. Relative errors of $(J/U)_c$ are less than 1% for $d=3$ and less than 2% for $d=2$.

g	$d=2$		$d=3$	
	$(\mu/U)_c$	$(J/U)_c$	$(\mu/U)_c$	$(J/U)_c$
1	0.376	5.909E-002	0.393	3.407E-002
2	1.427	3.480E-002	1.437	2.007E-002
3	2.448	2.473E-002	2.455	1.427E-002
4	3.460	1.920E-002	3.465	1.108E-002
5	4.470	1.569E-002	4.472	9.005E-003
10	9.483	8.208E-003	9.485	4.736E-003
20	19.491	4.202E-003	19.492	2.425E-003
50	49.496	1.706E-003	49.497	9.842E-004
100	99.498	8.571E-004	99.498	4.946E-004
1000	999.50	8.609E-005	999.50	4.968E-005
10 000	9999.50	8.613E-006	9999.50	4.970E-006

with limiting values (0.345 for $d=2$ and 0.299 for $d=3$) falling significantly above the mean-field prediction of $1/4$, which follows from Eq. (13). Even for $d=10$, the data still exceed the mean-field result by 4%.

To conclude, the diagrammatic many-body perturbation theory based on Kato's series (7), though impractical to work out analytically in high orders, becomes a powerful and accurate tool when turned into a numerically executable algorithm. The merit of this technique rests not only in the fact

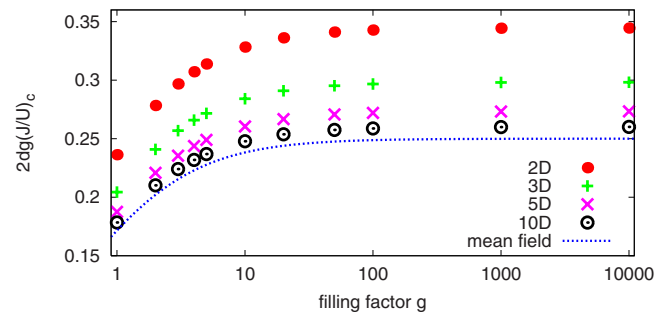


FIG. 4. (Color online) Critical product $2dg(J/U)_c$ for $d=2, 3, 5$, and 10 vs g , together with the mean-field limit. Even for $d=10$, the large g limit still exceeds the mean-field prediction by 4%.

that it enables one to access regimes which could not be reached before, such as experimentally important filling factors $g > 1$ (Ref. 1) or the crossover to the quantum rotor dynamics depicted in Fig. 4, but also in its great flexibility. For instance, with appropriately constructed diagrams it also yields correlation functions. Thus, the applicability of this approach is by no means exhausted by the present calculation of the Bose-Hubbard phase diagram.

We thank F. Gebhard and A. Pelster for insightful discussions and B. Capogrosso-Sansone for providing the QMC data (Refs. 7 and 8). Computer power was obtained from the GOLEM I cluster of the Universität Oldenburg. N.T. acknowledges support from the Studienstiftung des deutschen Volkes. A.E. thanks M. Lewenstein for kind hospitality and acknowledges a Feodor Lynen research grant from the Alexander von Humboldt foundation.

*teichmann@theorie.physik.uni-oldenburg.de

- ¹I. Bloch, J. Dalibard, and W. Zwerger, *Rev. Mod. Phys.* **80**, 885 (2008).
- ²M. P. A. Fisher, P. B. Weichman, G. Grinstein, and D. S. Fisher, *Phys. Rev. B* **40**, 546 (1989).
- ³D. Jaksch, C. Bruder, J. I. Cirac, C. W. Gardiner, and P. Zoller, *Phys. Rev. Lett.* **81**, 3108 (1998).
- ⁴M. Greiner, O. Mandel, T. Esslinger, T. W. Hänsch, and I. Bloch, *Nature (London)* **415**, 39 (2002).
- ⁵A. Eckardt, C. Weiss, and M. Holthaus, *Phys. Rev. Lett.* **95**, 260404 (2005).
- ⁶A. Zenesini, H. Lignier, D. Ciampini, O. Morsch, and E. Arimondo, arXiv:0809.0768, *Phys. Rev. Lett.* (to be published).
- ⁷B. Capogrosso-Sansone, N. V. Prokof'ev, and B. V. Svistunov, *Phys. Rev. B* **75**, 134302 (2007).
- ⁸B. Capogrosso-Sansone, Ş. G. Söyler, N. Prokof'ev, and B. Svistunov, *Phys. Rev. A* **77**, 015602 (2008).
- ⁹J. K. Freericks and H. Monien, *Phys. Rev. B* **53**, 2691 (1996).
- ¹⁰N. Elstner and H. Monien, *Phys. Rev. B* **59**, 12184 (1999).
- ¹¹T. D. Kühner, S. R. White, and H. Monien, *Phys. Rev. B* **61**, 12474 (2000).

- ¹²C. Kollath, U. Schollwöck, J. von Delft, and W. Zwerger, *Phys. Rev. A* **69**, 031601(R) (2004).
- ¹³C. Kollath, A. M. Läuchli, and E. Altman, *Phys. Rev. Lett.* **98**, 180601 (2007).
- ¹⁴T. Kato, *Prog. Theor. Phys.* **4**, 514 (1949).
- ¹⁵A. Eckardt, arXiv:0811.2353 (unpublished).
- ¹⁶S. Sachdev, *Quantum Phase Transitions* (Cambridge University Press, Cambridge, England, 1999).
- ¹⁷D. van Oosten, P. van der Straten, and H. T. C. Stoof, *Phys. Rev. A* **67**, 033606 (2003).
- ¹⁸C. Bruder, R. Fazio, and G. Schön, *Ann. Phys.* **14**, 566 (2005).
- ¹⁹J. W. Negele and H. Orland, *Quantum Many-Particle Systems* (Westview, Reading, MA, 1998).
- ²⁰F. E. A. dos Santos and A. Pelster, *Phys. Rev. A* **79**, 013614 (2009).
- ²¹M. P. Gelfand, R. R. P. Singh, and D. A. Huse, *J. Stat. Phys.* **59**, 1093 (1990).
- ²²H. Kleinert, *Path Integrals in Quantum Mechanics, Statistics, Polymer Physics, and Financial Markets* (World Scientific, Singapore, 2006).